The Cryosphere Discuss., 9, 2543–2562, 2015
www.the-cryosphere-discuss.net/9/2543/2015/
doi:10.5194/tcd-9-2543-2015

The Cryosphere Discussions
Open Access

The benefit of using sea ice concentration satellite data products with uncertainty estimates in summer sea ice data assimilation

Q. Yang[1,2], M. Losch[2], S. Losa[2], T. Jung[2,3], L. Nerger[2], and T. Lavergne[4]

[1]National Marine Environmental Forecasting Center, Beijing, China
[2]Alfred Wegener Institute, Helmholtz Centre for Polar and Marine Research, Bremerhaven, Germany
[3]University of Bremen, Bremen, Germany
[4]Norwegian Meteorological Institute, Oslo, Norway

Received: 30 January 2015 – Accepted: 31 March 2015 – Published: 21 April 2015

Correspondence to: Q. Yang (qinghua.yang@awi.de)

Published by Copernicus Publications on behalf of the European Geosciences Union.

Abstract

We present sensitivity experiments in which the Ocean and Sea Ice Satellite Application Facility (OSISAF) near-real time sea ice concentration data and the recently released Sea Ice Climate Change Initiative (SICCI) data are assimilated during summer. The data assimilation system uses the MIT general circulation model (MITgcm) and a local Singular Evolutive Interpolated Kalman (LSEIK) filter. Atmospheric forcing uncertainties are modelled by using atmospheric ensemble forcing which is taken from the UK Met Office (UKMO) system available through the TIGGE (THORPEX Interactive Grand Global Ensemble) database. When a constant data uncertainty is assumed, the assimilation of SICCI concentrations outperforms the assimilation of OSISAF data in both concentration and thickness forecasts. This is probably because the SICCI data retrieval uses an improved processing algorithms and methodologies. For the assimilation of SICCI data, using the observation uncertainties that are provided with the data improves the ensemble mean state of ice concentration compared to using constant data errors, but does not improve the ice thickness. This is caused by a mismatch between the SICCI concentration and the modelled physical ice concentration. To account for this mismatch the SICCI product should feature larger uncertainties in summer. Consistently, thickness forecasts can be improved by raising the minimum observation uncertainty to inflate the underestimated data error and ensemble spread.

1 Introduction

For the past 30 years, the Arctic sea ice extent and volume consistently decreased in all seasons with a maximum decline in summer (IPCC, 2013). Arctic sea ice decline opens new economic opportunities such as shipping and tourism. Accurate summer sea ice forecasts are therefore urgently required to thoroughly manage the opportunities and risks associated with Arctic climate change (Eicken, 2013).

TCD
9, 2543–2562, 2015

Realistic initial model states are important for accurate sea ice prediction; hence sea ice data assimilation (DA) plays a pivotal role in sea ice forecasting. Data assimilation requires both reliable observed quantities and realistic uncertainty estimates. These requirements, especially regarding data uncertainties, are now also increasingly recognized by the sea ice remote sensing community. Previous studies have shown that the assimilation of sea ice concentration data can improve sea ice concentration estimates (e.g., Lisæter et al., 2003; Lindsay and Zhang, 2006; Stark et al., 2008; Tietsche et al., 2013; Buehner et al., 2014) and also summer sea ice thickness fields through cross-correlations between ice concentration and thickness (Yang et al., 2015a). Given that error estimates in previous efforts were assumed to be constant, there is scope for further improvement through the use of more realistic uncertainty estimates.

In 2010, the European Meteorological Satellite Agency (EUMETSAT) Ocean and Sea Ice Satellite Application Facility (OSISAF, www.osi-saf.org) released a climate data record of sea ice concentration based on SMMR and SSM/I data that covers the years 1978–2009 (Eastwood et al., 2011; Product OSI-409). This dataset features an explicit correction of the satellite signal due to atmosphere weather, dynamic adaptation of algorithm tie-points, and spatio-temporally varying maps of uncertainties. In fact, this OSI-409 dataset and its uncertainties were already successfully used for data assimilation purposes (e.g., Massonnet et al., 2013).

In May 2014, the European Space Agency (ESA)-Sea Ice Climate Change Initiative (SICCI) released a sea ice concentration data set with associated uncertainty estimates (Version 1.11) to the public. In many respects, the SICCI sea ice concentration dataset features an update of the algorithms and processing methodologies used for the OSISAF OSI-409 dataset and, importantly, revised uncertainty estimates (Lavergne and Rinne, 2014). Although the SSM/I time-series produced in SICCI, v1.11 is shorter than that of the OSI-409 (covering only 1992–2008), it includes sea ice concentration maps from AMSR-E (2002–2011), which were not available in the OSISAF OSI-409 dataset. This new data set provides an

TCD
9, 2543–2562, 2015

opportunity to study the effect of the revised local (i.e., spatially varying) uncertainties on the assimilation of sea ice concentration data, and hence sea ice prediction skill. In this study, we follow the approach of Yang et al. (2015a, b) by focusing on the summer of 2010 and using the same local ensemble-based Singular Evolutive Interpolated Kalman (LSEIK) filter (Pham et al., 1998; Pham, 2001). The purpose of the study is to quantify the impact of different uncertainty approximations on sea ice data assimilation through a comparison with independent ice concentration and ice thickness observations.

2 Forecasting experiment design

We use the MITgcm sea ice–ocean model (Marshall et al., 1997; Losch et al., 2010, 2014) Following Yang et al. (2015a, b), this study employs an Arctic regional configuration with a horizontal resolution of about 18 km and open boundaries in the North Atlantic and North Pacific (Losch et al., 2010; Nguyen et al., 2011). To explicitly include flow dependent uncertainty in atmospheric forcing, the approach by Yang et al. (2015a) was used in which UK Met Office (UKMO) ensemble forecasts from the TIGGE archive (THORPEX Interactive Grand Global Ensemble; http://tigge.ecmwf.int/) drive the ensemble of sea ice–ocean models. Each of the selected UKMO ensemble forecasts consists of one unperturbed "control" forecast and an ensemble of 23 forecasts with perturbed initial conditions. For further details the reader is referred to Bowler et al. (2008) and Yang et al. (2015a).

The simulated and satellite observed sea ice concentration are combined using a sequential SEIK filter with second order exact sampling (Pham et al., 1998; Pham, 2001) coded within the Parallel Data Assimilation Framework (PDAF, Nerger and Hiller, 2013; http://pdaf.awi.de). The SEIK filter algorithm is selected to assimilate the sea ice concentration because it is computationally efficient when applying with nonlinear models (Nerger et al., 2005). The filter algorithm includes the following

TCD
9, 2543–2562, 2015

phases: initialization, forecast, analysis and ensemble transformation. The sequence of forecast, analysis and ensemble transformation is repeated.

The required initial ensemble approximates the uncertainty in the initial state of the physical phenomena. Following Yang et al. (2015a), we used a model integration driven by the 24 h UKMO control forecasts over the period of 1 June to 31 August 2010 to estimate the initial state error covariance matrix of sea ice concentration and thickness. The leading Empirical Orthogonal Functions (EOFs) of the considered model variability are used to generate the initial ensemble of the sea ice state (concentration and thickness). An ensemble size of 23 states is chosen to match with the ensemble size of UKMO perturbed forcing. In the forecast phase, all ensemble states are dynamically evolved in time with the fully nonlinear sea ice model driven by the UKMO ensemble atmospheric forcing. The analysis step combines the predicted model state with the observational information and computes a corrected state every 24 h. The error covariance matrix and ensemble of model state are also updated. With the SEIK filter as a reduced-rank square-root approach, the updated ensemble samples the analyzed model uncertainties according to the leading EOFs.

The SEIK analysis is performed locally for each water column of the model surface grid by assimilating the observational information only within a radius of 126 km (~ 7 grid points). Within the radius, we weighted the observations assuming quasi-Gaussian (Gaspari and Cohn, 1999) dependence of the weights on the distance from the analyzed grid point (see Janjić et al., 2012). As the atmospheric errors are already explicitly accounted for by the ensemble forcing, an ensemble inflation simulating model errors is not needed in this LSEIK configuration (Yang et al., 2015a).

Three daily sea ice concentration data sets are used in this study. The SICCI fields from AMSR-E (Lavergne and Rinne, 2014) and the OSISAF fields from SSM/I (Product OSI-401-a; Eastwood et al., 2011) are used in the data assimilation, these products consist of daily fields provided on a 25 and 10 km polar stereographic grid, respectively. The two processed data sets come from different satellite sensors, and the SICCI uses more advanced algorithms and processing details, for example, SICCI

TCD
9, 2543–2562, 2015

uses a revised algorithm merging method and tunes the tie-points dynamically with a smaller time window than OSISAF (Lavergne and Rinne, 2014). In the SICCI data set, the North Pole data gap is filled by interpolation, and daily maps of total standard error (uncertainty) are provided. The ice concentration data used for evaluation are from the National Snow and Ice Data Center (NSIDC; Cavalieri and others, 2012; http://nsidc.org/data/docs/daac/nsidc0051_gsfc_seaice.gd.html). This product consists of daily fields with 25 km grid spacing. Note that NSIDC concentration for summer 2010 is derived from another passive microwave sensor SSMIS onboard DMSP F-17, so it is independent from the SICCI and OSISAF data used in the assimilation.

We compare our simulation results to measurements of sea ice draft from the Beaufort Gyre Experiment Program (BGEP) Upward Looking Sonar (ULS) moorings located in the Beaufort Sea (BGEP_2009A, BGEP_2009D; http://www.whoi.edu/beaufortgyre; see Fig. 1 for the locations). The error in ULS measurements of ice draft is estimated as 0.1 m (Melling et al., 1995) Drafts are converted to thickness by multiplying by a factor of 1.1 (Nguyen et al., 2011).

Following Yang et al. (2015a, b), in this study, the system's forecasting skills are evaluated with a series of 24 h forecasts over the period of 1 June–30 August 2010 during which the LSEIK filter is applied every day. During this summer melting period the Arctic sea ice extent (area with at least 15 % sea ice concentration) shrank from 11.8 million km^2 on 1 June to 5.3 million km^2 on 30 August 2010 (calculation from the NSIDC data). Although there are some difference between the SICCI and the OSISAF sea ice concentration, both data show a clear picture of sea ice melting in Arctic summer: on 1 June, most of the Arctic Ocean was covered with heavy sea ice, while on 30 August, the sea ice area was shrunk to the central Arctic and the concentration was also much reduced (Fig. 1); the open water was found in the interior pack ice near the North Pole as early as 12 July 2010 (NSIDC, http://nsidc.org/arcticseaicenews/2010/07/).

Four experiments, which mainly differ in the way uncertainties are represented, form the backbone of this study:

TCD
9, 2543–2562, 2015

1. LSEIK-1: OSISAF SSM/I sea ice concentration data were assimilated with a constant uncertainty value of 0.25 (one standard deviation). This constant uncertainty value is larger than the measurement error to account for a representation error.

2. LSEIK-2: SICCI sea ice concentration data were assimilated with a constant uncertainty value of 0.25. This experiment has the same configuration as LSEIK-1.

3. LSEIK-3: Same as LSEIK-2 but using the uncertainty fields provided with the SICCI product. A minimum uncertainty of 0.01 is imposed to avoid complications due to divisions by very small numbers.

4. LSEIK-4: Same as LSEIK-3, but with a minimum uncertainty of 0.10.

To reflect the uncertainties in the interpolated sea ice concentration from SICCI over the data-void North Pole, a constant uncertainty of 0.30 is used in this region for all experiments.

3 Results

Figure 2 compares the root mean square error (RMSE) for ensemble mean ice concentration forecasts with and without data assimilation with respect to independent NSIDC SSMIS ice concentration for the period 1 June–30 August 2010. As errors tend to be large for small ice concentrations, all RMSE are evaluated only at grid points where either the model or the observations have ice concentrations larger than 0.05 (Lisæter et al., 2003; Yang et al., 2015b).

All the data assimilation experiments reduce deviations of the forecasted ice concentration from the satellite-based data. Compared to the free run without data

TCD
9, 2543–2562, 2015

assimilation, mean RMSE of LSEIK-1, LSEIK-2, LSEIK-3 and LSEIK-4 ensemble mean forecasts are reduced from 0.24 to 0.13, 0.12, 0.09 and 0.11. Assimilating the SICCI data set with a constant uncertainty of 0.25, LSEIK-2 agrees better with the independent NSIDC observations during most of the time than LSEIK-1, which assimilates OSISAF with the same constant uncertainty. At all times, LSEIK-3 and LSEIK-4, using the SICCI-provided uncertainty estimates and adjusted minimum uncertainties, agree better with the independent NSIDC observations than LSEIK-2, which employs a constant uncertainty. Furthermore, it is worth pointing out that LSEIK-3, with the SICCI-provided uncertainties, agrees best with the independent NSIDC observations. This shows that the forecasting system produces a more realistic ensemble mean state for sea ice concentration when time and space dependent uncertainties provided with the satellite observations are used.

The time series of daily 24 h forecast of sea ice thickness are compared to in situ ULS-observations BGEP_2009A (Fig. 3a) and BGEP_2009D (Fig. 3b). Note, that the numerical model carries mean thickness (volume over area) as a variable. The observed thickness is multiplied by SICCI local ice concentration to arrive at the observed mean thickness shown in Fig. 3. At BGEP_2009A, the mean thickness on 1 June was about 2.5 m. With ice melting, the thickness was rapidly reduced in July, and reached about 0.2 m on 30 August. Similarly, the mean thickness at BGEP_2009D was about 3.5 m on 1 June and was reduced to less than 0.1 m on 30 August (Fig. 3). All forecasts with DA show improvements over the free-running MITgcm after late July. The ice thickness RMSE at BGEP_2009A has been reduced from 0.86 m in the free model run to 0.58 m in LSEIK-1, 0.46 m in LSEIK-2, 0.64 m in LSEIK-3, and 0.46 m in LSEIK-4. The RMSE at BGEP_2009D has been reduced from 0.93 m in the free model run to 0.85 m in LSEIK-1, 0.59 m in LSEIK-2, 0.55 m in LSEIK-3, and 0.62 m in LSEIK-4. Using the same constant uncertainty of 0.25, LSEIK-1 with assimilation of OSISAF data overestimates the mean ice thickness in July, while LSEIK-2 with assimilation of SICCI data agrees better with observations at both BGEP_2009A (Fig. 3a) and BGEP_2009D (Fig. 3b). By using the original SICCI uncertainty, LSEIK-3 gives a good agreement

TCD
9, 2543–2562, 2015

with the in situ observations at BGEP_2009D (Fig. 3b), but over-estimates the mean sea ice thickness at BGEP_2009A (Fig. 3a), especially from mid-July to mid-August. By imposing a minimum uncertainty of 0.10 in the original uncertainties, the LSEIK-4 thickness agrees better with the BGEP_2009A data, and is basically equivalent to LSEIK-2.

4 Discussion

Based on the OSISAF and the recently released SICCI sea ice concentration data that provides uncertainty estimates, a series of sensitivity experiments with different data error statistics has been carried out to test the impact of sea ice concentration uncertainties in data assimilation. Compared to a DA configuration with constant uncertainty of 0.25, the DA of SICCI data with provided uncertainties can give a better short-range ensemble mean forecasts for sea ice concentration in summer. For ice thickness forecasts the influence of observational uncertainties is ambiguous (beneficial in one case while seemingly detrimental in another).

The sensitivity of the data assimilation to the observation uncertainties can be explained by the employed (atmospheric) model and data error statistics in the LSEIK assimilation system. Although we have not directly included the model errors due to the possible suboptimal sea ice internal parameters, the ensemble forcing approach used here was shown to be very effective at representing model uncertainty associated with atmospheric forcing fields (Yang et al., 2015a). Data error is represented by the original observational data uncertainties of ice concentrations that are provided with the SICCI data set and are supposed to reflect errors in satellite retrievals and data processing. In Fig. 4, we show the provided observation uncertainties on 1 and 16 June, 1 and 16 July, 1 and 16 August 2010. Larger uncertainties up to 0.3 are present at the ice edge. However, for the summer sea ice pack the data uncertainties seem to be very low. For example, on 16 July 2010 when surface ice melting prevails and the satellite-based ice

TCD
9, 2543–2562, 2015

concentration estimates are known to underestimate the sea ice cover, the provided uncertainties at the sea ice pack area are still lower than 0.06 (Fig. 4d).

In fact, Lavergne and Rinne (2014, Sect. 2.2.1.1 “summer melt-ponding”) report that AMSR-E and SSM/I, like all other passive microwave sensors, cannot distinguish ocean water (in leads) from melt water (in ponds) because of the very shallow penetration depths of the microwave signal. Therefore, these radiometric sea ice concentrations are closer to one minus the open water fraction (ponds and leads), than to the physical sea ice concentration in our models. This point is further elaborated in Ivanova et al. (2015).

It is worth highlighting two important issues: first, even if the targeted quantity is not the physical ice concentration, the SICCI product should probably feature larger uncertainties in summer. Second, the mismatch between the measured and modelled quantities calls for a matching relation in form of an observation operator to be embedded in the data assimilation procedure. Given the scope of this study, the solution implemented in LSEIK-4, that is to enlarge the observation uncertainties using a minimum value of 0.10, is a pragmatic but effective approach.

The ensemble-represented SDs of sea ice concentration for LSEIK-3 turn out to be relatively small. For example, on 30 August 2010, most of the SDs in the Arctic central area and the sea ice edge area are less than 0.01 and 0.03, respectively (Fig. 5c). This means that all members are very close to the ensemble mean and the data assimilation will have only little effect. LSEIK-4 has a similar spread distribution pattern of higher SDs in the sea ice edge area and lower SDs in the concentrated central ice area but overall higher SDs than LSEIK-3. Together with the fact that LSEIK-3 does not fit the thickness observations as well as LSEIK-4, this suggests that the ensemble forecast spread for sea ice concentration is too low and cannot reflect the uncertainty. As only observations of sea ice concentration are assimilated, sea ice thickness is influenced indirectly during the data assimilation through the point-wise covariance between the ice concentration and thickness. Here, the very small sea ice concentration variance leads to a very small sea ice thickness spread (Fig. 6c). This may explain why the LSEIK-3 system is not very effective at improving the sea ice

TCD
9, 2543–2562, 2015

thickness estimates. However, by raising the minimum uncertainty to 0.10, which is meant to account for the mismatch between the observed and modelled quantities as well as the underestimated observation uncertainties, the ensemble spread of sea ice concentration is increased in LSEIK-4. The increased spread in the sea ice concentration allows the system to better represent the uncertainties and leads to a larger ice thickness spread (Fig. 6d). The sea ice thickness forecasts are improved accordingly.

5 Conclusions

In this study, we assimilate OSISAF and SICCI sea ice concentration data during the summer period. While the OSISAF data is assimilated with a constant data uncertainty, and the summer SICCI sea ice concentration data takes into account the data uncertainties provided by the distributors. Even with a constant data uncertainty for the SICCI data, its assimilation results in better estimates of the sea ice concentration and thickness. This is expected because the retrieval of SICCI concentration data uses an improved algorithms and processing methodologies (Lavergne and Rinne, 2014). The estimates are further improved when the SICCI-provided uncertainty estimates are taken into account. However, it was found that our data assimilation system cannot give a reasonable ensemble spread of sea ice concentration and thickness if we use the provided uncertainty directly. This is because (1) there is a mismatch between the sea ice concentration as observed by the passive microwave sensors (radiometric concentration) and that simulated by our model (physical concentration), and (2) the provided observation uncertainties are probably underestimated. A simple and pragmatic approach appears to correct this by imposing a minimum threshold value on the provided uncertainties in summer. We finally note that the mismatch between the observed and modelled ice concentration (radiometric vs. physical) does not exist in winter when there is no surface melting, and that fully resolving the mismatch in

TCD
9, 2543–2562, 2015

summer calls for more research, for example by considering melt-pond schemes, and observation operators.

Acknowledgements. We thank ESA's Sea Ice Climate Change Initiative (SICCI), the OSISAF High Latitude Processing Centre and the National Snow and Ice Data Center (NSIDC) for providing the ice concentration data, as well as the Woods Hole Oceanographic Institution for the provision of sea ice draft data. The UKMO ensemble forecasting data were accessed through the TIGGE data server in European Centre for Medium-Range Weather Forecasts (ECMWF). This study is supported by the BMBF (Federal Ministry of Education and Research, Germany) – SOA (State Oceanic Administration, China) Joint Project (01DO14002), the National Natural Science Foundation of China (41 376 005, 41 376 188), and the China Scholarship Council. We thank the editor for constructive comments that helped improve the manuscript.

References

Bowler, N., Arribas, A., Mylne, K., Robertson, K., and Beare, S.: The MOGREPS short-range ensemble prediction system, Q. J. Roy. Meteor. Soc., 134, 703–722, doi:10.1002/qj.234, 2008.

Buehner, M., Caya, A., Carrieres, T., and Pogson, L.: Assimilation of SSMIS and ASCAT data and the replacement of highly uncertain estimates in the Environment Canada Regional Ice Prediction System, Q. J. Roy. Meteor. Soc., doi:10.1002/qj.2408, online first, 2014.

Cavalieri, D. J., Parkinson, C. L., DiGirolamo, N., and Ivanoff, A.: Intersensor calibration between F13 SSMI and F17 SSMIS for global sea ice data records, IEEE T. Geosci. Remote, 9, 233–236, 2012.

Eastwood, S., Larsen, K. R., Lavergne, T., Neilsen, E., and Tonboe, R.: OSI SAF Global Sea Ice Concentration Reprocessing: Product User Manual, Version 1.3., available at: http://osisaf.met.no (last access: October 2013), 2011.

Eicken, H.: Ocean science: arctic sea ice needs better forecasts, Nature, 497, 431–433, 2013.

Gaspari, G. and Cohn, S. E.: Construction of correlation functions in two and three dimensions, Q. J. Roy. Meteor. Soc., 125, 723–757, 1999.

IPCC: Climate Change 2013: The Physical Science Basis, Contribution of Working Group I to the Fifth Assessment Report of the Intergovernmental Panel on Climate Change, edited by:

TCD
9, 2543–2562, 2015

Stocker, T. F., Qin, D., Plattner, G. K. et al., Cambridge University Press, Cambridge, UK, New York, NY, USA, 1535 pp., 2013.
Ivanova, N., Pedersen, L. T., Tonboe, R. T., Kern, S., Heygster, G., Lavergne, T., Sørensen, A., Saldo, R., Dybkjær, G., Brucker, L., and Shokr, M.: Satellite passive microwave measurements of sea ice concentration: an optimal algorithm and challenges, The Cryosphere Discuss., 9, 1269–1313, doi:10.5194/tcd-9-1269-2015, 2015.
Janjić, T., Nerger, L., Albertella, A., Schröter, J., and Skachko, S.: On domain localization in ensemble based Kalman filter algorithms, Mon. Weather Rev., 139, 2046–2060, 2011.
Lavergne, T. and Rinne, E.: Sea Ice Climate Change Initiative Phase 1: D3.4 Product User Guide (PUG), version 2.0., available at: http://icdc.zmaw.de/, last access: May 2014.
Lindsay, R. W. and Zhang, J.: Assimilation of ice concentration in an ice–ocean model, J. Atmos. Ocean. Tech., 23, 742–749, 2006.
Lisæter, K. A., Rosanova, J., and Evensen, G.: Assimilation of ice concentration in a coupled ice–ocean model, using the Ensemble Kalman filter, Ocean Dynam., 53, 368–388, 2003.
Losa, S., Danilov, S., Schröter, J., Nerger, L., Maßmann, S., and Janssen, F.: Assimilating NOAA SST data into the BSH operational circulation model for the North and Baltic Seas: inference about the data, J. Marine Syst., 105–08, 152–162, 2012.
Losch, M., Menemenlis, D., Campin, J. M., Heimbach, P., and Hill, C.: On the formulation of sea-ice models, Part 1: effects of different solver implementations and parameterizations, Ocean Model., 33, 129–144, 2010.
Losch, M., Fuchs, A., Lemieux, J., and Vanselow, A.: A parallel Jacobian-free Newton–Krylov solver for a coupled sea ice–ocean model, J. Comput. Phys., 257, 901–911, doi:10.1016/j.jcp.2013.09.026, 2014.
Marshall, J., Adcroft, A., Hill, C., Perelman, L., and Heisey, C.: A finite-volume, incompressible Navier Stokes model for studies of the ocean on parallel computers, J. Geophys. Res., 102, 5753–5766, 1997.
Massonnet, F., Mathiot, P., Fichefet, T., Goosse, H., König Beatty, C., Vancoppenolle, M., and Lavergne, T.: A model reconstruction of the Antarctic sea ice thickness and volume changes over 1980–2008 using data assimilation, Ocean Model., 64, 67–75, 2013.
Melling, H., Johnston, P. H., and Riedel, D. A.: Measurements of the underside topography of sea ice by moored subsea sonar, J. Atmos. Ocean. Tech., 12, 589–602, 1995.
Nerger, L. and Hiller, W.: Software for ensemble-based data assimilation systems – implementation strategies and scalability, Comput. Geosci., 55, 110–118, 2013.

TCD
9, 2543–2562, 2015

Nerger, L., Hiller, W., and Schröter, J.: A comparison of error subspace Kalman filters, Tellus A, 57, 715–735, 2005.
Nerger, L., Danilov, S., Hiller, W., and Schröter, J.: Using sea-level data to constrain a finite-element primitive-equation ocean model with a local SEIK filter, Ocean Dynam., 56, 634–649, 2006.
Nguyen, A. T., Menemenlis, D., and Kwok, R.: Arctic ice–ocean simulation with optimized model parameters: approach and assessment, J. Geophys. Res., 116, C04025, doi:10.1029/2010JC006573, 2011.
Pham, D.: Stochastic methods for sequential data assimilation in strongly nonlinear systems, Mon. Weather Rev., 129, 1194–1207, 2001.
Pham, D. T., Verron, J., and Gourdeau, L.: Filtres de Kalman singuliers évolutif pour l'assimilation de données en océnographie, Compt. Rend. Acad. Sci. Terre Planètres, 326, 255–260, 1998 (in French).
Stark, J. D., Ridley, J., Martin, M., and Hines, A.: Sea ice concentration and motion assimilation in a sea ice–ocean model, J. Geophys. Res., 113, C05S91, doi:10.1029/2007JC004224, 2008.
Tietsche, S., Notz, D., Jungclaus, J. H., and Marotzke, J.: Assimilation of sea-ice concentration in a global climate model – physical and statistical aspects, Ocean Sci., 9, 19–36, doi:10.5194/os-9-19-2013, 2013.
Yang, Q., Losa, S. N., Losch, M., Jung, T., and Nerger, L.: The role of atmospheric uncertainty in Arctic sea ice data assimilation and prediction, Q. J. Roy. Meteor. Soc., doi:10.1002/qj.2523, online first, 2015a.
Yang, Q., Losa, S. N., Losch, M., Liu, J., Zhang, Z., Nerger, L., and Yang, H.: Assimilating summer sea ice concentration into a coupled ice–ocean model using a localized SEIK filter, Ann. Glaciol., 56, 38–44, doi:10.3189/2015AoG69A740, 2015b.

TCD
9, 2543–2562, 2015

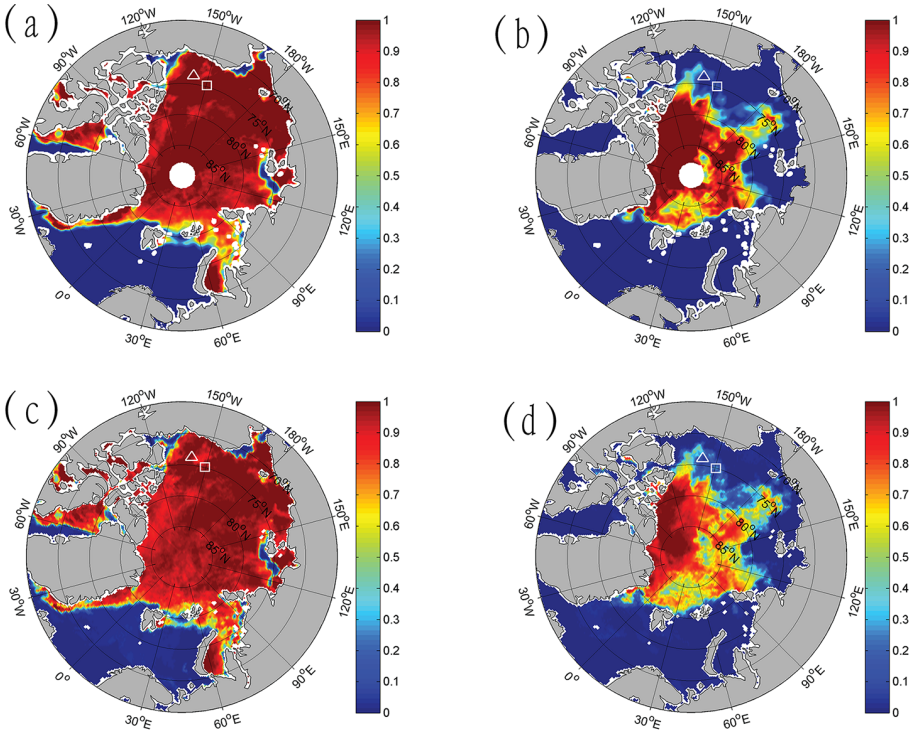

Figure 1. The OSISAF (OSI-401-a; **a, b**) and SICCI **(c, d)** sea ice concentration on 1 June **(a, c)** and 30 August 2010 **(b, d)**. The locations of BGEP_2009A and BGEP_2009D are shown as a square with white line and a triangle with white line, respectively.

TCD
9, 2543–2562, 2015

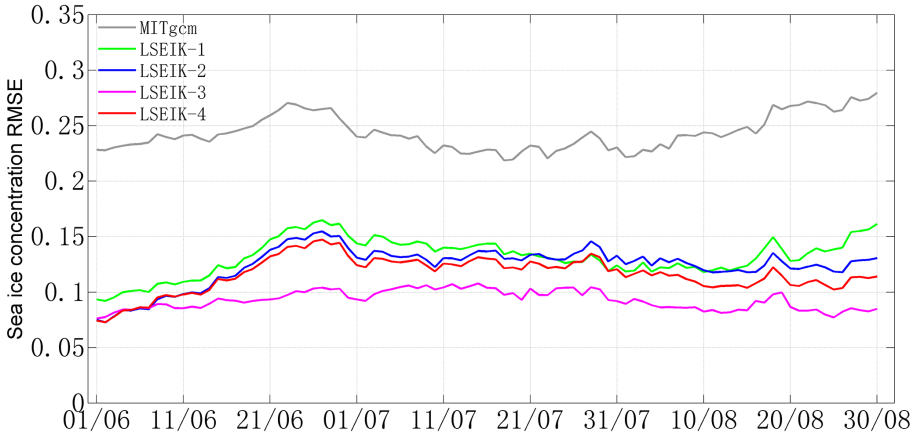

Figure 2. Temporal evolution of RMSE differences between sea ice concentration forecasts and the independent NSIDC SSMIS ice concentration data. The RMSE of the MITgcm free-run, LSEIK-1, LSEIK-2, LSEIK-3 and LSEIK-4 24 h forecasts are shown as gray, green, blue, magenta and red solid lines, respectively.

TCD
9, 2543–2562, 2015

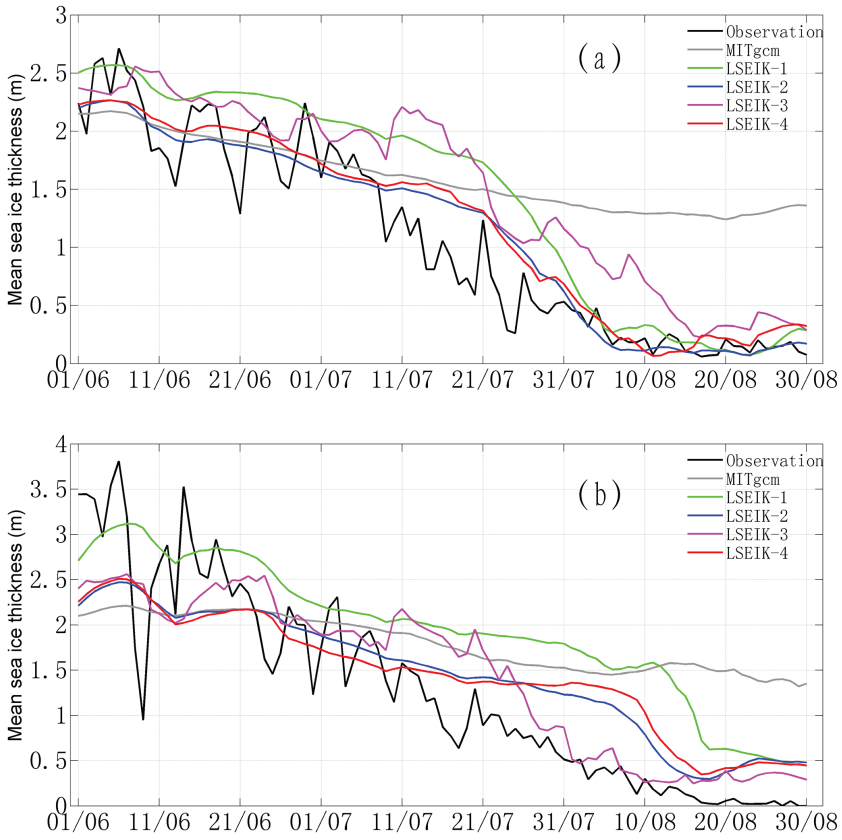

Figure 3. Evolution of mean sea ice thickness (m) at **(a)** BGEP_2009A and **(b)** BGEP_2009D Beaufort Sea from 1 June to 30 August 2010. The black solid lines show the obtained mean ice thickness observations. The MITgcm free-run, LSEIK-1, LSEIK-2, LSEIK-3 and LSEIK-4 24 h ice thickness forecasts are shown as green, blue, magenta and red solid lines, respectively.

TCD
9, 2543–2562, 2015

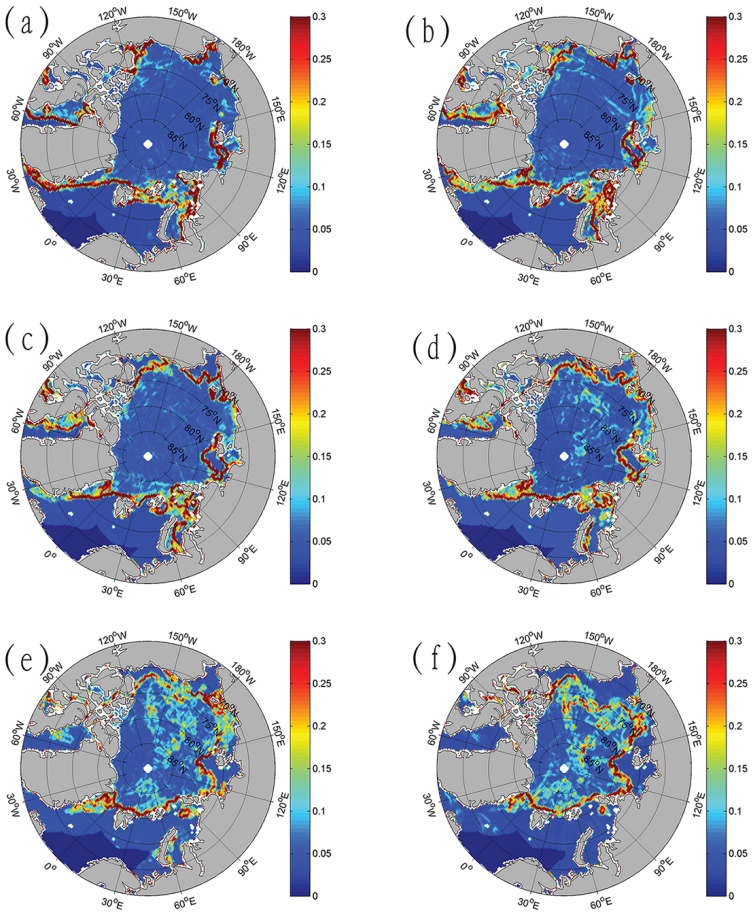

Figure 4. The SICCI sea ice concentration uncertainty on **(a)** 1 June, **(b)** 16 June, **(c)** 1 July, **(d)** 16 July, **(e)** 1 August and **(f)** 16 August 2010.

TCD
9, 2543–2562, 2015

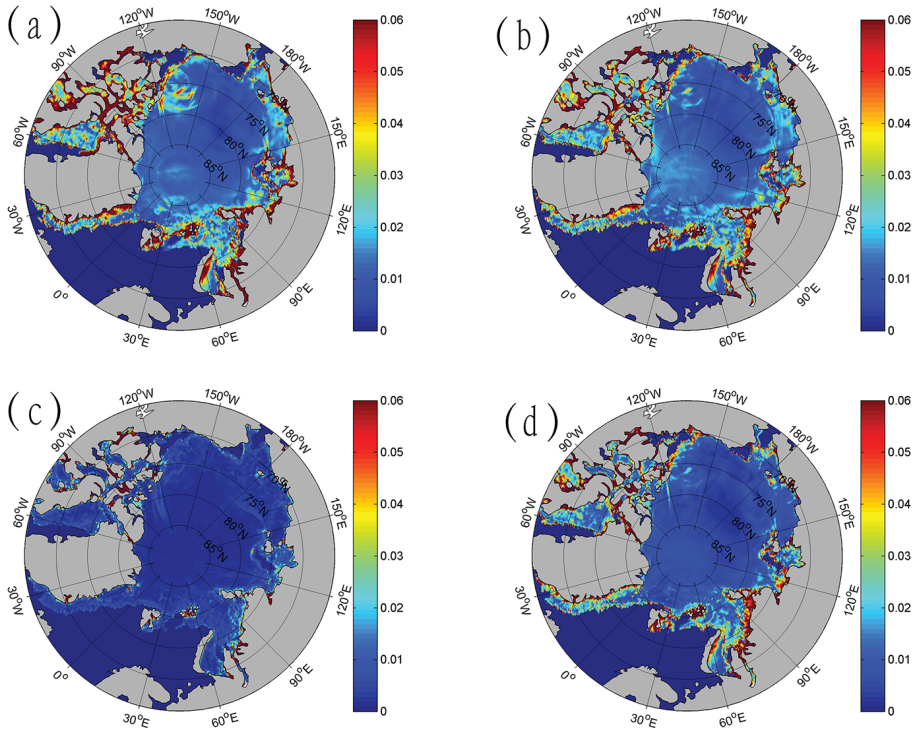

Figure 5. Sea ice-concentration SD for the individual grid cells as calculated from the 24 h ensemble forecasts on 30 August 2010. **(a)** LSEIK-1, **(b)** LSEIK-2, **(c)** LSEIK-3 and **(d)** LSEIK-4.

TCD
9, 2543–2562, 2015

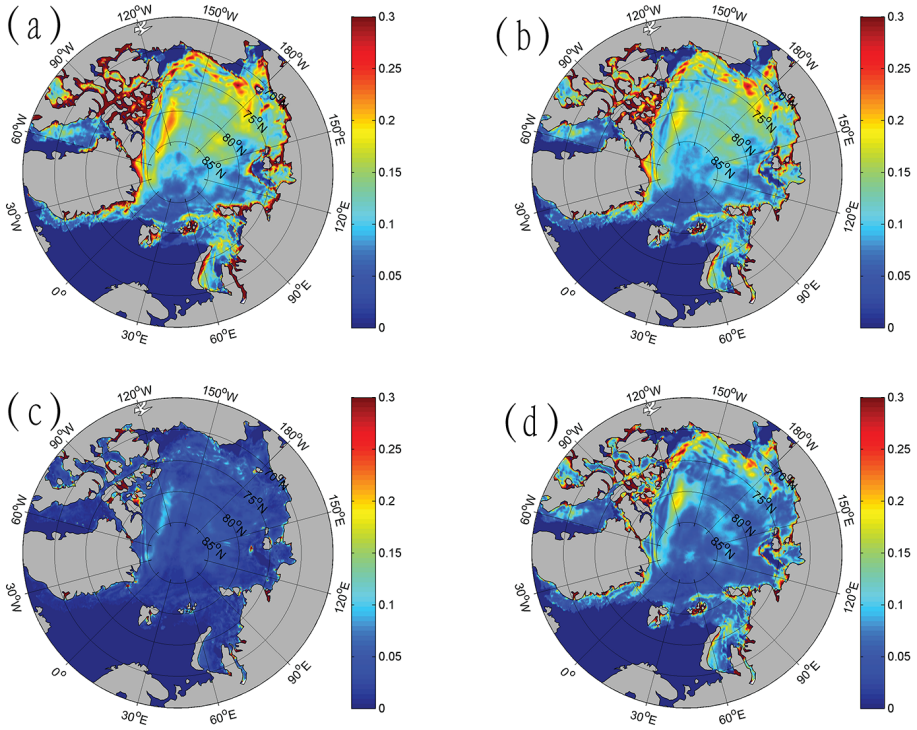

Figure 6. Sea ice thickness SD for the individual grid cells as calculated from the 24 h ensemble forecasts on 30 August 2010. **(a)** LSEIK-1, **(b)** LSEIK-2, **(c)** LSEIK-3 and **(d)** LSEIK-4.

TCD
9, 2543–2562, 2015